# ($\eta^3$-Phenylallyl)(phosphanyloxazoline)palladium Complexes: X-Ray Crystallographic Studies, NMR Investigations, and Ab Initio/DFT Calculations**

**Martin Kollmar,[a] Henning Steinhagen,[a] Jörg. P. Janssen,[a] Bernd Goldfuss,[a, d] Svetlana A. Malinovskaya,[a] Jordi Vázquez,[a] Frank Rominger,[a] and Günter Helmchen*[a]**

*Dedicated to Professor Lutz F. Tietze on the occasion of his 60th birthday*

**Abstract:** All possible ($\eta^3$-allyl)palladium complexes (**1**–**4**) of the ligand (4*S*)-[2-(2′-diphenylphosphanyl)phenyl]-4,5-dihydro-4-(2-propyl)-oxazole (**L1**) and $\eta^3$-allyl ligands with one to three phenyl substituents at the terminal allylic centers were synthesized and characterized by X-ray crystal structure analysis and, with respect to allylic isomers, by NMR investigations. Equilibrium geometries, electronic structures, and relative energies of isomeric complexes were computed by restricted Hartree–Fock (RHF) and density functional theory (DFT) calculations; experimentally determined isomer ratios could be reproduced. The results allowed important conclusions to be drawn regarding the mechanism of Pd-catalyzed asymmetric allylic substitutions.

**Keywords:** ab initio calculations · allyl ligands · NMR spectroscopy · palladium · structure elucidation

## Introduction

Pd-catalyzed enantioselective C–C and C–N bond-forming allylic substitution reactions are frequently employed in organic synthesis.[1] Scheme 1 describes two important classes of allylic substitutions that can be carried out enantioselectively with chiral catalysts. Phosphanyloxazolines,[2] modular

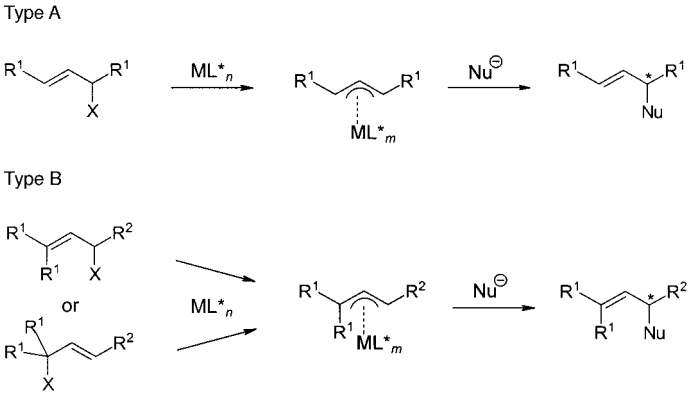


Scheme 1. Important classes of allylic substitutions that can be carried out enantioselectively with chiral catalysts (M = Pd).

$C_2$-diphosphines,[3] and phosphanylmyrtanic acids[4] are presently most broadly employed as chiral ligands. The two latter types are particularly useful for cyclic substrates.

We have systematically studied ($\eta^3$-allyl)Pd complexes of phosphanyloxazolines by X-ray crystal structure analysis, determined solution structures by NMR techniques, and compared the results with those from ab initio and DFT calculations. Recently, our results obtained with 1,3-dialkylallyl derivatives of type A were published as Part 1 of this series of articles.[5] In the present article, Part 2 of the series, our results on a complete series of ($\eta^3$-arylallyl)Pd complexes of both type A and type B are presented. Whilst complexes of type A have been studied extensively, little information is available on complexes of type B. We regard this report as the

[a] Prof. Dr. G. Helmchen, Dr. M. Kollmar,[+] Dr. H. Steinhagen,[++] Dr. J. P. Janssen, Prof. Dr. B. Goldfuss,[+++] Dr. S. A. Malinovskaya, Dr. J. Vázquez, Dr. F. Rominger
Organisch-chemisches Institut der Universität Heidelberg
Im Neuenheimer Feld 270, 69120 Heidelberg (Germany)
Fax: (+49) 6221-54-4205
E-mail: mako@nmr.mpibpc.mpg.de
en4@popix.urz.uni-heidelberg.de

[+] Dr. M. Kollmar
New address: Max-Planck Institut für Biophysikalische Chemie
Abteilung NMR basierte Strukturbiologie
Am Fassberg 11, 37077 Göttingen (Germany)

[++] Dr. H. Steinhagen
New address: Bayer AG, Pharma, PH-R-CR CWL
42096 Wuppertal (Germany)
E-mail: henning.steinhagen.hs@bayer-ag.de

[+++] Prof. Dr. B. Goldfuss
New address: Institut für Organische Chemie
Universität zu Köln
Greinstrasse 4, 50939 Köln (Germany)

[**] (Phosphanyloxazoline)palladium Complexes, Part II. Part I see: ref. [5].

Supporting information (tables of positional parameters for all computed isomers of complex **1**) for this article is available on the WWW under http://wiley-vch.de/home/chemistry/ or from the author.

  0947-6539/02/0814-3103 $ 17.50+.50/0 

direct sequel of Part 1 and, therefore, only the most pertinent definitions of structural parameters as well as the literature references concerning general aspects of X-ray structures, NMR investigations, and quantum-chemical calculations are repeated here.

Rationalization of the steric course and enantioselectivity of a reaction of type A requires knowledge about the ratio of the intermediate ($\eta^3$-allyl)palladium complexes and their relative rates and regioselectivities of substitution (cf. Scheme 2). In most (but not all) cases, isomer interconversion

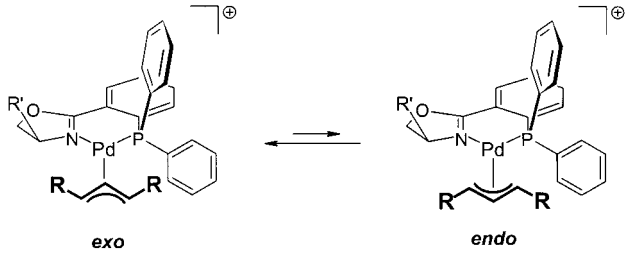


Scheme 2. *exo*–*endo* isomerism of ($\eta^3$-allyl)palladium complexes containing a PHOX ligand.

is faster than the addition of a nucleophile; thus, the Curtin–Hammett principle applies. In the case of alkyl derivatives, up to six isomers were found (*exo-endo* and *syn*,*anti* isomers), whereas for 1,3-diaryl derivatives, only the *exo*,*syn*,*syn* (preferred) and *endo*,*syn*,*syn* isomers were observed. Generally, for ($\eta^3$-allyl)(PHOX)palladium complexes, *exo* isomers are more stable than *endo* isomers. We have previously argued[6] that this preference is caused by repulsive interactions between the group R and the pseudoequatorial P-phenyl group, as schematically depicted in Scheme 3. In the following, the validity of this argument will be strongly supported by experimental data.

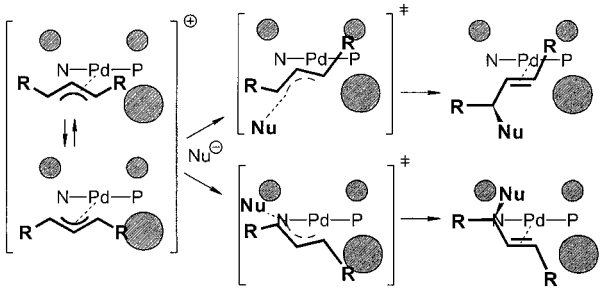

Scheme 3. Mechanistic aspects of the allylic substitution. The (PHOX)Pd fragment, in the conformation as in Scheme 2, is schematically described by the N-Pd-P fragment and the shaded circles which represent the equatorial (large) and axial phenyl groups at P and the group R′. The upper pathway leads to the preferred enantiomer.

The two dominant transition states of the reaction are schematically described in Scheme 3. These transition states arise from preferred attack of the nucleophile at the allylic terminal carbon *trans* to phosphorus.[6, 7] There is ample information on the starting allyl complexes; however, information on product olefin complexes is scarce.[8] Quantum-chemical calculations on the transition state, which are so far limited to simple model systems and amines as nucleophiles,[9] as well as solvent effects[10] on *exo-endo* ratios of $\eta^3$-allyl complexes and enantioselectivities indicate a late transition state. The importance of this point should not be overestimated because, as apparent from the description in Scheme 3, the structural change along the reaction path of the allylic moiety relative to the (PHOX)Pd fragment is small and this fragment is fairly rigid and its structure insensitive to changes in the allyl group, as was demonstrated in Part 1. Accordingly, many structural features of the ($\eta^3$-allyl)palladium complex are preserved in the transition state and, therefore, studies of structures and isomer distributions of ($\eta^3$-allyl)palladium complexes are important.

An obvious feature of the reaction is the rotation of the allylic moiety along the reaction path. In several allyl complexes it was observed that, even in the crystal, their allylic moiety was rotated in the same direction as in the course of the substitution reaction.[7, 10b] Scheme 3 immediately illustrates that this direction of rotation is to be expected in order to minimize steric interactions.[11] It was speculated that the direction and degree of rotation in the allyl ligand in palladium complexes of N,P ligands determines the rate and enantioselectivity of the reaction.[7] To shed additional light on this issue, we have taken particular care in the analysis of the rotational state of the allylic moiety and investigated the energy surface of rotation and tilting of the allyl ligand by quantum-chemical calculations.

Finally, it must be emphasized that the above considerations refer to N,P ligands and similar ligands with two different donor centers. Differing aspects have to be invoked for ($\eta^3$-allyl)palladium complexes of $C_2$-symmetric ligands which, in spite of symmetry breaking, are not expected to generally display clear structural properties, namely differing bond lengths of allylic terminal carbon atoms to palladium, to explain the regioselectivity of nucleophilic attack.

## Results

### Preparation of the ($\eta^3$-allyl)palladium complexes

Complexes **1**–**4** and *ent*-**5** were prepared from known[12] ($\eta^3$-allyl)palladium chloride dimer complexes (Scheme 4). The latter were obtained from the corresponding allylic alcohols in excellent yields according to the procedure of Bosnich et al.,[12] which was also previously employed for the preparation of ($\eta^3$-alkylallyl)palladium complexes (Part I[5]). Reactions with ligands **L1** or **L3** and either silver perchlorate, silver hexafluoroantimonate, or silver hexafluorophosphate in $CH_2Cl_2$/methanol furnished complexes **1**–**4** and *ent*-**5**.[13] Crystals suitable for X-ray diffraction were obtained from their solutions in dichloromethane by slow evaporation of the solvent or by introducing *n*-hexane or diethyl ether by diffusion. The crystal structure of complex **2** was already published in 1994;[6b] in the course of the present work, crystals of superior quality were obtained and a substantially improved structure was determined.[14]

### Crystal structures

The structures of complexes **1**–**4** and *ent*-**5** were determined by X-ray crystallography. Crystallographic data and parameters are listed in Table 1.[15] Complexes **2**–**4** and *ent*-**5** crystallized as *exo* isomers and gave structures of high quality.



0947-6539/02/0814-3104 $ 17.50+.50/0 *Chem. Eur. J.* **2002**, *8*, No. 14

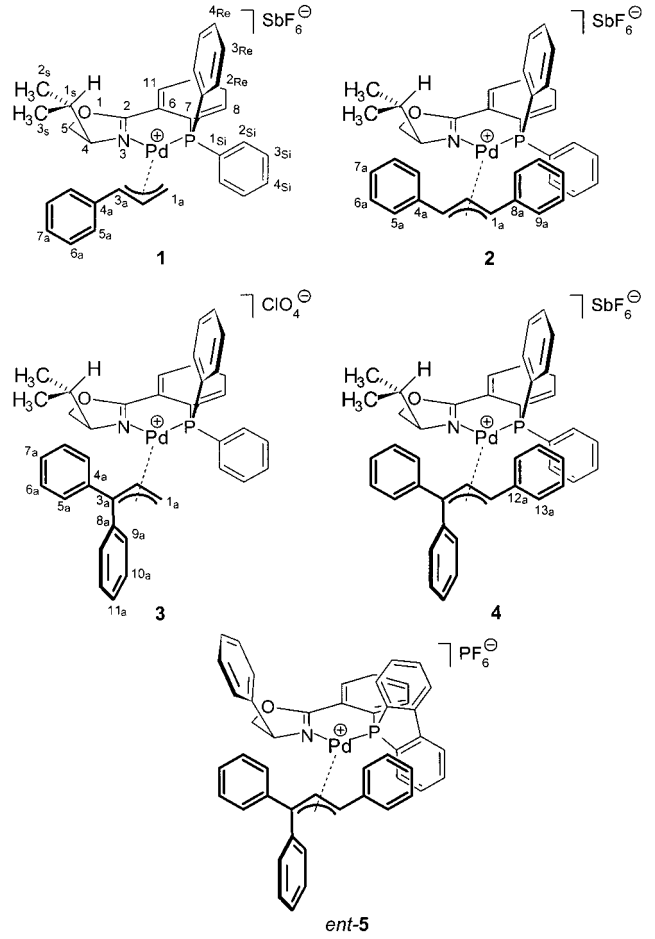


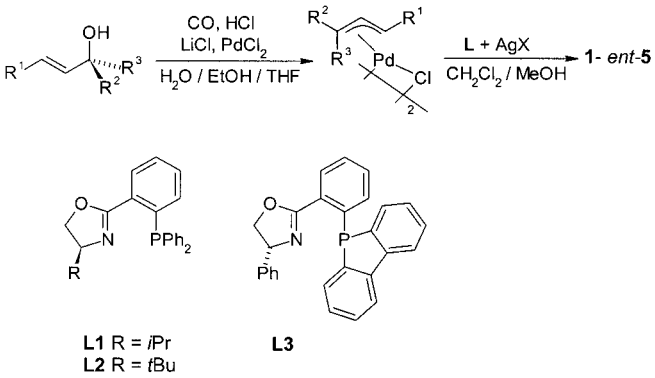





Scheme 4. Preparation of ($\eta^3$-allyl)palladium complexes.

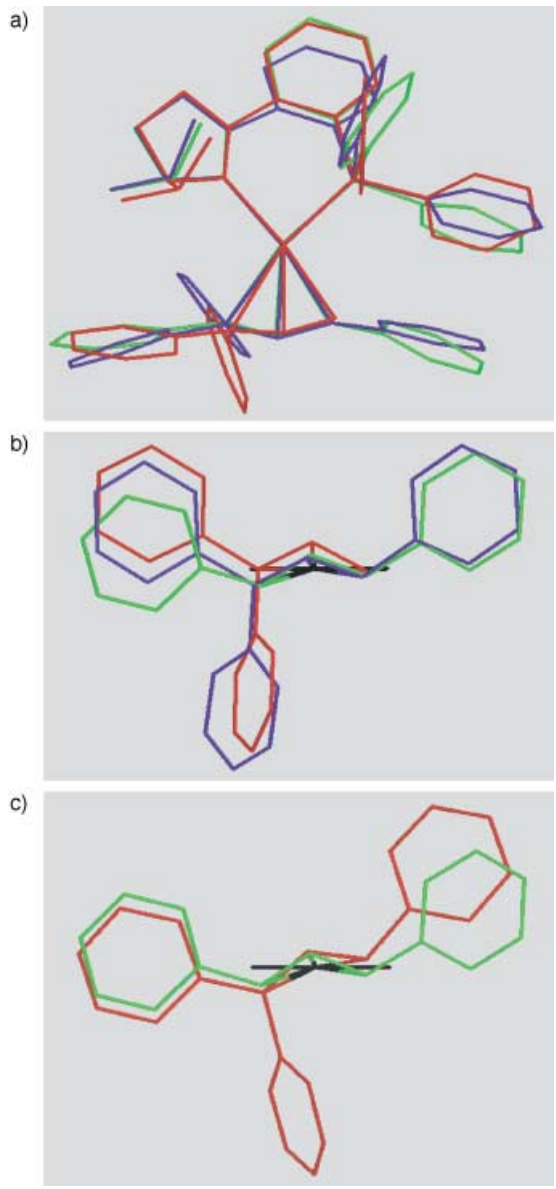


Figure 1. Superpositions of crystal structures of the ($\eta^3$-allyl)palladium complexes with best fit of the coordination plane [N,Pd,P]. The anions and hydrogen atoms were omitted for clarity. In b) and c) the coordination plane [N,Pd,P] is indicated by the horizontal black line, with N being located at the left. a) Top view of complexes **2** (green), **3** (red), and 4 (blue). b) Allyl groups of complexes **2** (green), **3** (red), and **4** (blue). c) Allyl groups of complexes **2** (green) and *ent*-**5** (red).

Complex **4** showed two crystallographically independent molecules in the asymmetric unit which were evaluated separately. Complex **1** crystallized as a 7:3 mixture of the *endo* and the *exo* isomer. The positions of the allyl atoms $C2_a$ and $C3_a$ could be refined independently for the *endo* and the *exo* form, whereas the rest of the molecule is very similar for both isomers. (cf. footnote [a] in Table 2). Crystal structures of complexes **2**–**5** and **1** are displayed in Figure 1 and Figure 4, respectively.

**[N,Pd,P] moieties**: Bond lengths and angles describing the moiety [N,Pd,P] are listed in Table 2 and Figure 2. Data of (1,3-dialkylallyl)palladium complexes[5] are also presented in Figure 2 for comparison. The lengths of the Pd–N bonds ($2.111 \pm 0.015$ Å) and Pd–P bonds ($2.274 \pm 0.008$ Å) are very similar for all complexes and are in the expected range.[5, 16, 17] The bond angle N-Pd-P is found in the narrow range of $88.3 \pm 1.5^\circ$. Because of the small variation of geometric parameters, the [N,Pd,P] plane was used as the *reference plane* for the description of the geometry and position of the phosphanyldihydrooxazole and the allyl ligand.

**Allyl moieties**: The Pd–C bonds *trans* to phosphorus ($Pd–C3_a$, $2.311 \pm 0.053$ Å) are longer by 0.186 Å, on average, than the Pd–C bonds *trans* to nitrogen ($Pd–C1_a$, $2.125 \pm 0.030$ Å) (Table 3). The average value is somewhat misleading because the differences are spread over a wide range, from

Table 1. Crystallographic data for complexes **1**–**5**.

| | **1** | **2** | **3** | **4** | **5** |
|---|---|---|---|---|---|
| Formula | $C_{33}H_{33}F_6NOPPdSb$ | $C_{39}H_{37}F_6NOPPdSb$ | $C_{39}H_{37}ClNO_5PPd$ | $C_{45}H_{41}F_6NOPPdSb \cdot 0.5\,(C_2H_5)_2O$ | $C_{48}H_{37}F_6NOP_2Pd$ |
| $M_W$ | 832.72 | 908.82 | 772.52 | 1021.97 | 926.19 |
| $T$[K] | 200(2) | 123(2) | 200(2) | 200(2) | 293(2) |
| $\lambda$[Å] | 0.71073 | 0.71073 | 0.71073 | 0.71073 | 0.71069 |
| crystal system | monoclinic | tetragonal | monoclinic | orthorhombic | monoclinic |
| space group | $P2_1$ | $P4_3$ | $P2_1$ | $P2_12_12_1$ | $P2_1$ |
| $Z$ | 2 | 4 | 2 | 8 | 2 |
| $a$[Å] | 9.6058(1) | 11.3530(1) | 9.6082(2) | 13.5975(2) | 10.142(3) |
| $b$[Å] | 19.2842(3) | 11.3530(1) | 15.2944(3) | 15.2128(2) | 15.119(3) |
| $c$[Å] | 9.7598(1) | 28.6891(3) | 11.9458(2) | 42.8358(2) | 13.697(4) |
| $\alpha$[°] | 90 | 90 | 90 | 90 | 90 |
| $\beta$[°] | 113.9767(4) | 90 | 100.665(1) | 90 | 104.06(2) |
| $\gamma$[°] | 90 | 90 | 90 | 90 | 90 |
| $V$[Å$^3$] | 1651.90(4) | 3697.76(6) | 1725.13(6) | 8860.8(2) | 2037.3(9) |
| $\rho_{calcd}$[g cm$^{-3}$] | 1.674 | 1.632 | 1.487 | 1.532 | 1.510 |
| $\mu$[mm$^{-1}$] | 1.471 | 1.322 | 0.707 | 1.114 | 0.600 |
| $T_{max}/T_{min}$ | 0.77/0.63 | 0.80/0.65 | 0.97/0.90 | 0.86/0.72 | |
| crystal form | irregular | fragment | polyhedron | irregular | |
| crystal size[mm$^{-1}$] | $0.38 \times 0.23 \times 0.22$ | $0.42 \times 0.23 \times 0.22$ | $0.25 \times 0.10 \times 0.06$ | $0.50 \times 0.42 \times 0.25$ | |
| $2\theta_{max}$[°] | 51.16 | 54.92 | 51.14 | 51.21 | 62.52 |
| no. of reflns | 7675 | 26656 | 13015 | 41377 | 8845 |
| no. of indep. reflns | 4235 | 8388 | 5714 | 14895 | 8529 |
| no. of obs. reflns ($I > 2\sigma(I)$) | 4162 | 8388 | 5064 | 14309 | 7801 |
| restraints/parameters | 12/426 | 1/465 | 1/447 | 0/1072 | 1/538 |
| GoF on $F^2$ | 1.06 | 1.083 | 0.99 | 1.14 | 1.07 |
| final $R$ | 0.019 | 0.019 | 0.027 | 0.026 | 0.039 |
| final $R_w$ | 0.048 | 0.044 | 0.048 | 0.067 | 0.099 |
| max/min in diff. map[e Å$^{-3}$] | 0.35/ − 0.37 | 0.40/ − 0.43 | 0.28/ − 0.31 | 1.10/ − 0.95 | 0.77/ − 0.39 |

Table 2. Selected bond lengths[Å] and bond angles[°] of the phenylallyl complexes **1**–**5**.

| Complex | **1** (*endo*)[a] | **2** (*exo*) | **3** (*exo*) | **4**$^{\mathbf{A}}$ (*exo*)[b] | **4**$^{\mathbf{B}}$ (*exo*)[b] | *ent*-**5** (*exo*) |
|---|---|---|---|---|---|---|
| Pd−N | 2.101(3) | 2.096(2) | 2.116(3) | 2.119(3) | 2.122(3) | 2.126(3) |
| Pd−P | 2.2663(8) | 2.2668(5) | 2.2690(9) | 2.281(1) | 2.272(1) | 2.267(1) |
| Pd−C1$_a$ | 2.096(4) | 2.137(2) | 2.095(4) | 2.130(4) | 2.154(4) | 2.131(4) |
| Pd−C2$_a$ | 2.176(9) | 2.184(2) | 2.169(3) | 2.180(4) | 2.174(4) | 2.184(4) |
| Pd−C3$_a$ | 2.318(5) | 2.258(2) | 2.364(3) | 2.304(4) | 2.282(4) | 2.295(3) |
| C1$_a$−C2$_a$ | 1.409(8) | 1.420(3) | 1.412(5) | 1.413(6) | 1.419(6) | 1.425(6) |
| C2$_a$−C3$_a$ | 1.390(9) | 1.393(3) | 1.397(5) | 1.405(5) | 1.406(6) | 1.400(5) |
| N-Pd-P | 88.51(8) | 88.92(5) | 88.23(7) | 86.93(9) | 89.19(9) | 89.86(9) |
| C1$_a$-Pd-C3$_a$ | 66.9(2) | 66.75(8) | 66.4(1) | 68.6(1) | 68.1(1) | 68.0(1) |
| C1$_a$-C2$_a$-C3$_a$ | 121.3(7) | 118.7(2) | 121.8(3) | 125.2(4) | 123.3(4) | 122.6(4) |

[a] Complex **1** crystallized as a 7:3 mixture of the *endo* and the *exo* isomer. The positions of the allyl atoms C2$_a$ and C3$_a$ could be refined independently for the *endo* and the *exo* form, whereas the rest of the molecule is very similar for both isomers. The accuracy of the obtained geometry for the allyl region is affected by this disorder, the uncertainty of the results may be greater than the given standard deviation. The hydrogen atoms could be refined freely for the pyramidalized atom C1$_a$, all other hydrogen atoms were taken into account at calculated positions. [b] The unit cell of this crystal structure contains two crystallographically independent cations which are denoted **4**$^{\mathbf{A}}$ and **4**$^{\mathbf{B}}$.

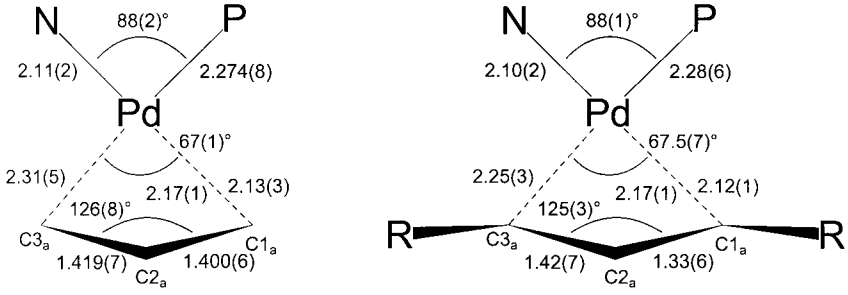


Figure 2. Average bond lengths and angles of the Pd coordination plane and the allyl system. Left: Phenylallyl complexes; right: alkylallyl complexes.

0.121 Å in complex **2** up to 0.269 Å in the (1,1-diphenylallyl)palladium complex **3**. Thus, differing steric interactions between the phenyl groups bound to the allyl moiety and the ligand are apparent. Variations of the angle C1$_a$-Pd-C3$_a$, 67.4 ± 1.2°, and the ligand bite angles N-Pd-P, 88.6 ± 1.7°, are small.

As found for the 1,3-dialkylallyl complexes,[5] the bonds C2$_a$−C3$_a$ are longer by 0.018 ± 0.010 Å than the bonds C1$_a$−C2$_a$. The angles C1$_a$-C2$_a$-C3$_a$ are 121 ± 3° and are thus similar to those observed in other $\eta^3$-allyl complexes. The location of the allylic moiety relative to the coordination plane is described by the tilt angle $\alpha$,[5] the angle between planes [C1$_a$,C2$_a$,C3$_a$] and [N,Pd,P], and by the dihedral angle $\tau$(N-P-C1$_a$-C3$_a$)[5] assessing the twist of the allylic group (Table 3). Similar to the 1,3-dialkylallyl complexes, values of angle $\alpha$, 115 ± 7°, of the phenylallyl complexes are spread over a wide range.

  0947-6539/02/0814-3106 $ 17.50+.50/0 *Chem. Eur. J.* **2002**, *8*, No. 14

Table 3. Selected structural parameters (angles[°], distances[Å]), describing the allyl ligand in relation to the [N,Pd,P] reference plane.

| Complex | **1** *endo* | **2** *exo* | **3** *exo* | **4**$^{A}$ [a] *exo* | **4**$^{B}$ [a] *exo* | *ent*-**5** *exo* |
|---|---|---|---|---|---|---|
| $\alpha$[b] | 118.7(7) | 118.5(2) | 106.9(3) | 122.1(4) | 121.4(4) | 116.6(2) |
| distance of $C1_a$ to the plane[N,Pd,P][c] | 0.065(7) | −0.183(3) | −0.002(5) | −0.169(5) | −0.164(5) | 0.163(5) |
| distance of $C2_a$ to the plane[N,Pd,P][c] | −0.246(9) | 0.331(3) | 0.665(4) | 0.285(5) | 0.218(5) | 0.335(4) |
| distance of $C3_a$ to the plane[N,Pd,P][c] | 0.601(6) | −0.407(2) | 0.023(4) | −0.358(4) | −0.526(4) | −0.618(4) |
| $\tau$ (N-P-$C1_a$-$C3_a$) | −12.9(2) | 5.30(9) | −0.6(2) | 4.2(2) | 8.4(2) | 18.7(1) |

[a] The unit cell of this crystal structure contains two crystallographically independent cations which are denoted **4**$^{A}$ and **4**$^{B}$. [b] Angle between the planes [N,Pd,P] and [$C1_a$,$C2_a$,$C3_a$]. [c] Atoms in the *Re* and *Si* half spaces of the plane [N,Pd,P] are defined to have positive and negative distances, respectively.

With respect to the twist of the allylic moiety, limiting situations are a trihapto allyl system ($\tau = 0°$) and a dihapto-bound olefinic system ($\tau \approx 28°$). The smallest twist angle ($\tau = -0.6°$) is found for the 1,1-diphenylallyl complex **3**. In this complex, the distances of $< 0.025$ Å (Table 3) of the terminal allylic carbon atoms, $C1_a$ and $C3_a$, to the [N,Pd,P] plane additionally demonstrate almost exactly planar coordination which is surprising for such a strongly asymmetrically substituted allyl system. The largest twist angle is displayed by the (1,1,3-triphenylallyl)palladium complex *ent*-**5** ($\tau = 18.7°$) which contains a phospholane ligand (cf. Figure 1c). In contrast, the two independent molecules of the (1,1,3-triphenylallyl)palladium complex **4** display $\tau = 4.2°$ and 8.4°. Finally, the *endo* allyl system in complex **1** is markedly tilted in the opposite direction ($\tau = -12.9°$) which was not observed for any other ($\eta^3$-allyl)(phosphanyldihydrooxazole)palladium complex. In conclusion, there is no apparent correlation between the magnitude and sign of the twist angle $\tau$ with structural features; accordingly, the potential energy surface with respect to tilt and twist of the allyl group is flat and lattice forces determine the actual values of parameters $\alpha$ and $\tau$ in the crystals.

**Conformation of the PHOX ligand**: The conformation of the PHOX ligand in the complexes was analyzed with parameters previously defined in our report on (1,3-dialkylallyl)palladium complexes (Part 1).[5] The results are presented in Table 4. Values of all the parameters are in the range observed for ($\eta^3$-1,3-dialkylallyl)palladium complexes and there is no systematic variation in relation to the substitution pattern of the allyl group. A clear example is provided by the two crystallographically independent molecules of complex **4** which display significantly differing conformers. In conclusion, the conformation of the dihydrooxazole moiety is strongly influenced by crystal packing forces.

## 2D-NMR investigation of the ($\eta^3$-allyl)palladium complexes

The solution structures of all complexes were analyzed with 2D NMR methods.[18] The nuclei were assigned according to the strategy previously outlined for ($\eta^3$-1,3-dialkylallyl)palladium complexes in Part 1[5] with the help of $^1$H,$^1$H-DQF-COSY, $^1$H,$^1$H-TOCSY, $^1$H,$^1$H-NOESY, $^1$H,$^{13}$C-HMBC-, and $^1$H,$^{13}$C-HSQC spectra. Complexes **3** and **4** each displayed a single compound which was identified as the *exo* isomer, that is, the same compound as found in the crystals.

As previously reported,[6b] complex **2** displays a 8:1 ratio of *exo* and *endo* isomers in THF solution.[19] Complex **1** crystallized as a 7:3 mixture of the *endo*,*trans* isomer **1nt** and the *exo*,*trans* isomer **1xt** (Figure 3). The solution of this compound displayed four sets of signals which we were able to assign to the four isomers described in Figure 3. Structures were assigned with the help of NOESY spectra and by analyzing the $^3J(3_a\text{-H,P})$ coupling constants.[14, 20]

The ratio of the isomers of complex **1** in $CD_2Cl_2$ was determined to be **1xt** (*exo*,*trans*):**1nt** (*endo*,*trans*):**1xc** (*exo*,*cis*):**1nc** (*endo*,*cis*) = 57.5:38:3.5:1. The marked preference for the *trans* isomers was expected on the basis of the argument (see the Introduction) that steric repulsion between the equatorial phenyl group bound to P and the phenyl group of the allylic moiety destabilizes the *cis* isomers. The complete absence of *cis* isomers in complexes **3** and **4** provides further strong support for this interpretation. In addition, the almost equipopulation of the isomers **1xt** and **1nt** clearly shows that the ratio of *exo* and *endo* isomers is governed by steric effects with regards to the equatorial phenyl group at P. The ratio of the isomers **1xc** and **1nc** (3.5:1) corresponds to the ratio 6:1 for isomers **2x** and **2n**, taking the necessarily low precision of the former value into account.

It was of interest to investigate the dynamic properties of complex **1**. 2D NOESY spectroscopy ($\tau_{mix} = 600$ ms, 254 K) of complex **1** showed exchange peaks between protons of isomers **1xt** and **1nt** (Scheme 5); there was no exchange with any of the *cis* isomers. The rate

Table 4. Selected structural parameters (angles[°], distances[Å]) describing the conformation of the PHOX ligand relative to the plane [N,Pd,P].

| Complex | **1** *endo* | **2** *exo* | **3** *exo* | **4**$^{A}$ [a] *exo* | **4**$^{B}$ [a] *exo* | *ent*-**5**[b] *exo* |
|---|---|---|---|---|---|---|
| $\chi$[c] | 36.8(1) | 33.08(8) | 32.6(1) | 41.7(1) | 34.9(1) | 28.33(1) |
| deviation from planarity[d] | 0.089 | 0.074 | 0.085 | 0.099 | 0.089 | 0.110 |
| $\phi$[e] | 67.9(1) | 51.8(1) | 70.02(8) | 45.4(1) | 62.80(9) | |
| N-P-$C1_{Re}$ | 95.6(1) | 100.19(8) | 95.6(1) | 92.6(1) | 100.8(1) | |
| N-P-$C1_{Re}$-$C2_{Re}$ | 84.4(3) | 50.4(2) | 86.4(3) | 69.2(3) | 54.1(3) | |
| $\psi$[f] | 50.1(4) | 64.05(6) | 49.8(2) | 40.1(3) | 53.2(2) | |
| N-P-$C1_{Si}$ | 158.4(1) | 151.53(9) | 157.4(1) | 162.3(1) | 152.2(2) | |
| N-P-$C1_{Si}$-$C2_{Si}$ | −9.7(6) | 20.6(3) | −2.5(5) | 26.2(7) | 15.4(5) | |

[a] The unit cell of this crystal structure contains two crystallographically independent cations which are denoted **4**$^{A}$ and **4**$^{B}$. [b] Because of the completely differing characteristics of the $PPh_2$ and the dibenzophospholanyl groups, the parameters describing the latter were not determined. [c] Angle between the "best-fit" plane through the ligand atoms N, C2, C6, C7, and P and the plane [N,Pd,P]. [d] Average of distances of the atoms N, C2, C6, C7, and P to the "best-fit" plane through them. [e] Torsion angle Pd-N-P-$C1_{Re}$. [f] Torsion angle Pd-N-P-$C1_{Si}$.

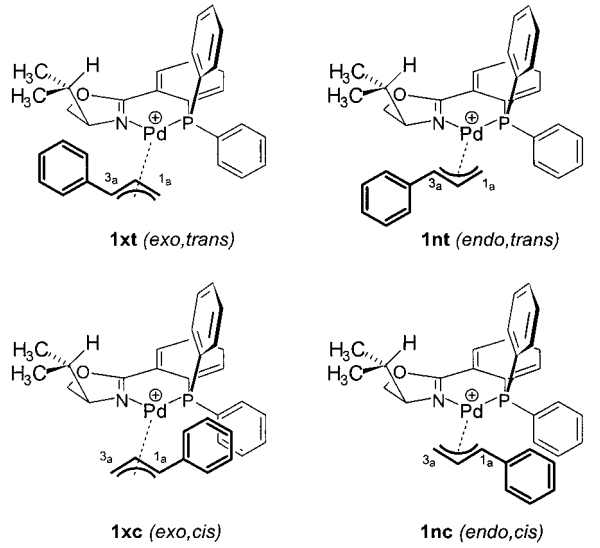


Figure 3. Schematic representation of the four isomers of complex **1** found in $CD_2Cl_2$ solution.[21]

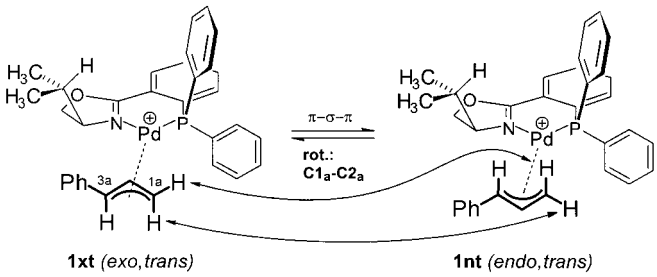


Scheme 5. Exchanging protons of isomers **1xt** and **1nt**.

constant, $k_{exch.} = 0.68$ Hz, was determined with methods that related cross- and diagonal-peak intensities. Of the[22] various interconversion modes discussed in Part 1, a $\eta^3$-$\eta^1$-$\eta^3$ rearrangement best explains the exchange pattern. This process involves opening of the Pd–$C3_a$ bond of **1xt** to give an intermediate $\eta^3$-allyl complex, preferred rotation around its single bond $C1_a$–$C2_a$, and reformation of the $\eta^3$-allyl complex **1nt**. No exchange among the minor isomers was found, probably as a result of the relatively low intensity.

## Ab Initio and DFT computations of geometries and relative energies

Quantum-chemical calculations have been widely applied to allyl palladium complexes (for reviews, see ref. [9]) and excellent results have been achieved on the aspects of isomer distributions[5, 23] and substitution reactions (transition-state structure,[24] regioselectivity, and [25] electronic substituent effects[26]).

Complex **1**, displaying as four different isomers in solution and in addition providing X-ray crystal data, was the most interesting target for quantum-chemical calculations. The relative energies of the four isomers were evaluated with the software package *Gaussian 98*.[27] All geometries were preoptimized by means of the Restricted Hartree–Fock (RHF) method with the 3-21G basis set for C, H, N, and O and with the LanL2DZ-ECP basis set for the P and Pd atoms.[28] In addition, refined geometry optimizations of the complexes were performed with the B3LYP hybrid DFT method[29] employing the LanL2DZ-ECP for Pd and P atoms and the 3-21G basis set for all other atoms. Solvent effects were assessed by computing single point energies at the B3LYP level (LanL2DZ-ECP for P, Pd and 3-21G* for C, H, N, and O) by means of the integral equation formalism polarized continuum model (IEF-PCM)[30] with dichloromethane as the solvent. The results are summarized in Table 5. The optimized calculated structure and the X-ray crystal structure are compared in Figure 4.

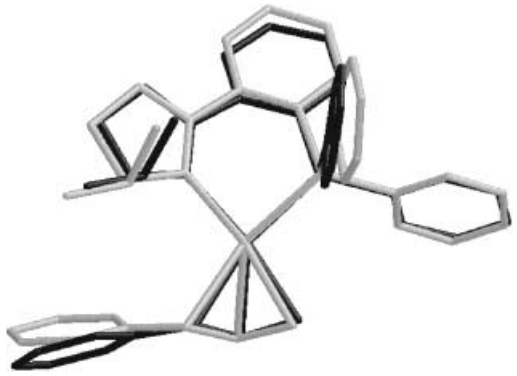

Figure 4. Superposition of structures of complex **1** obtained by X-ray structure analysis (black) and B3LYP optimization (gray).

All computations correctly favored the *trans* over the *cis* isomer and the *exo,cis* over the *endo,cis* isomer by $\approx 2$ kcal mol$^{-1}$. Figure 5 illustrates the position of the $1_a$-phenyl group relative to the equatorial phenyl group on phosphorus. This relationship is perhaps best characterized as pseudostaggered and pseudoeclipsed for the *exo* and *endo* isomer, respectively.

Not surprisingly, the very small energy difference between the *trans* isomers, experimentally $\approx 0.3$ kcal mol$^{-1}$ in $CD_2Cl_2$

Table 5. Total [a.u.] and relative [kcal mol$^{-1}$] energies for the four computed isomers of complex **1**.

| | RHF[a] | | B3LYP[b] | | B3LYP IEFPCM ($CH_2Cl_2$)[c] | | |
|---|---|---|---|---|---|---|---|
| Isomer | $E_{tot}$ | $E_{rel}$ | $E_{tot}$ | $E_{rel}$ | $E_{tot}$ | $E_{rel}$ | NMR ($CD_2Cl_2$) [%] |
| *exo,trans* | −1522.45933 | 0.00 | −1532.76521 | 0.00 | −1532.81085 | 0.00 | 57.5 |
| *endo,trans* | −1522.45958 | −0.16 | −1532.76522 | −0.01 | −1532.81043 | +0.26 | 38.0 |
| *exo,cis* | −1522.45561 | +2.33 | −1532.76121 | +2.51 | −1532.80647 | +2.75 | 3.5 |
| *endo,cis* | −1522.45252 | +4.27 | −1532.75823 | +4.38 | −1532.80401 | +4.29 | 1.0 |

[a] Method and basis set: B3LYP//RHF/LanL2DZ + ECP(P,Pd),3–21G(C,H,N,O). [b] Method and basis set: B3LYP/LanL2DZ + ECP(P,Pd),3–21G(C,H,N,O)//RHF/LanL2DZ + ECP(P,Pd),3–21G(C,H,N,O). [c] Method and basis set: IEFPCM-B3LYP/LanL2DZ(P,Pd),3–21G*(C,H,N,O)//RHF/LanL2DZ + ECP(P,Pd),3–21G(C,H,O,N).



0947-6539/02/0814-3108 $ 17.50+.50/0 *Chem. Eur. J.* **2002**, *8*, No. 14

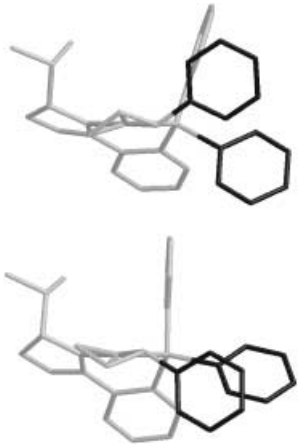

Figure 5. Calculated structures of isomers **1xc** (left) and **1nc** (right). The coordination plane is perpendicularly arranged relative to the plane of the paper, with N to the left. The equatorial phenyl group at P and the phenyl group of the phenylallyl ligand are emphasized.

solution, is not exactly reproduced by the calculations referring to the vacuum. However, by application of the solvent model ($CH_2Cl_2$ solution), the correct order and magnitude, 0.26 kcal mol$^{-1}$, is obtained. This result underlines the value of these calculations as information on the equilibrium geometries are only available (from the crystal structure analysis) for the *endo*,*trans* isomer.

Similar results were obtained for complex **2** (Table 6). Using the B3LYP hybrid DFT method[29] employing the

Table 6. Total ([a.u.]) and relative ([kcal mol$^{-1}$]) energies for the four computed isomers of complex **2**.

| | B3LYP[a] | | B3LYP IEFPCM ($CHCl_3$)[b] | | |
|---|---|---|---|---|---|
| Isomer | $E_{tot}$ | $E_{rel}$ | $E_{tot}$ | $E_{rel}$ | NMR ($CDCl_3$) [%][19] |
| *exo* | −1762.55586 | 0.0 | −1762.59471 | 0.0 | 86 |
| *endo* | −1762.55252 | +2.1 | −1762.59081 | +2.4 | 14 |

[a] Method and basis set: B3LYP/LanL2DZ + ECP(P,Pd),3–21G(C,H,N,O)//RHF/LanL2DZ + ECP(P,Pd),3–21G(C,H,N,O). [b] Method and basis set: IEFPCM-B3LYP/LanL2DZ(P,Pd),3–21G*(C,H,N,O)//RHF/LanL2DZ + ECP(P,Pd),3–21G(C,H,O,N).

LanL2DZ-ECP for Pd and P atoms and the 3-21G basis set for all other atoms an energy difference of 2.1 kcal mol$^{-1}$ was calculated for the *exo* and *endo* isomer (gas phase), correctly favoring the *exo* isomer as the more stable one. This result is in excellent agreement with NMR data.[19] Furthermore, the energy difference is very close to that (1.9 kcal mol$^{-1}$) found for the *cis*,*exo* and *cis*,*endo* isomers of complex **1**. This supports our previous conclusion that the isomer stabilities are mainly dominated by steric interactions with the equatorial P-bound phenyl group.

We have reported that tilting and twisting of the allyl group relative to the coordination plane, described by the angle $\alpha$ (the angle between planes [$C1_a$,$C2_aC3_a$] and [N,Pd,P]) and the torsion angle $\tau$(N-P-$C1_a$-$C3_a$) of alkylallyl complexes varies considerably ($\alpha = 120 \pm 5^\circ$, $\tau = 5 \pm 5^\circ$).[5] Variations of these parameters ($\alpha = 115 \pm 7^\circ$ and $\tau = 3 \pm 15^\circ$) are even more pronounced for the phenylallyl complexes. There is no apparent dependence of either of these angles on the steric bulk of the substituents at the oxazoline or the allyl group. This indicated a flat energy minimum with respect to these parameters. Computational assessment of the energy as a function of the tilt and twist angle was carried out for the exemplary allyl complex shown in Figure 6.

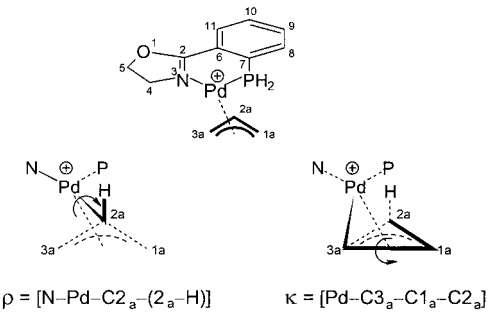


Figure 6. Model complex for assessing energies of twisting and tilting of the allyl group of the PHOX ligands. Twisting and tilting of the $\eta^3$-allyl group are described by torsion angles $\rho$(N-Pd-$C2_a$-$2_a$-H) and $\kappa$(Pd-$C3_a$-$C1_a$-$C2_a$), respectively.

For this assessment, torsion angles $\kappa$(Pd-$C3_a$-$C1_a$-$C2_a$) and $\rho$(N-Pd-$C2_a$-($2_a$-H)], respectively, were chosen as geometric parameters (cf. Figure 6). These angles are not completely independent of each other as are $\alpha$ and $\tau$ (cf.[5]), nevertheless, they give a good indication of the energetic cost of tilting and twisting of the allyl group. Values of the optimized structure of the model complex are $\rho = -77.0^\circ$ and $\kappa = 111.2^\circ$. A grid with 49 structures with fixed values of $\rho$ and $\kappa$ was calculated and an energy map (Figure 7) was derived by linear interpolation (Table 7).

The potential energy surface contains a flat minimum as anticipated. Structures with $\Delta\rho = 25-30^\circ$ and $\Delta\kappa = 12^\circ$ are located within an energy boundary of only 0.6 kcal mol$^{-1}$. The crystal structures of the alkylallyl and phenylallyl complexes are all found in this domain. Accordingly, values of these parameters are strongly influenced by crystal packing effects. Clearly, the regioselectivity of attack of a nucleophile at the allylic group can not be correlated with twisting, or in other words the rotational state, of the allyl group in the solid state.

Table 7. Relative energies ([kcal mol$^{-1}$]) of the minimization for a given pair of dihedral angles $\kappa$ and $\rho$.[a]

| | $\rho$ | | | | | | |
|---|---|---|---|---|---|---|---|
| $\kappa$ | −105° | −90° | −80° | −75° | −70° | −60° | −45° |
| 90° | +8.0 | +6.1 | +5.3 | +5.2 | +5.2 | +5.8 | +8.2 |
| 100° | +4.0 | +2.1 | +1.5 | +1.4 | +1.5 | +2.2 | +4.8 |
| 105° | +2.9 | +1.1 | +0.5 | +0.4 | +0.5 | +1.3 | +4.0 |
| 110° | +2.4 | +0.6 | +0.0 | 0.0 | +0.2 | +1.0 | +3.8 |
| 115° | +2.4 | +0.6 | +0.2 | +0.2 | +0.3 | +1.3 | +4.2 |
| 120° | +2.9 | +1.2 | +0.8 | +0.8 | +1.0 | +2.0 | +5.0 |
| 130° | +5.2 | +3.6 | +3.4 | +3.5 | +3.8 | +4.9 | +8.1 |

[a] Method and basis set: B3LYP/LanL2DZ + ECP(P,Pd),3–21G(C,H,N,O)//B3LYP/LanL2DZ + ECP(P,Pd),3–21G(C,H,N,O). No parameters were restricted except the two dihedral angles.

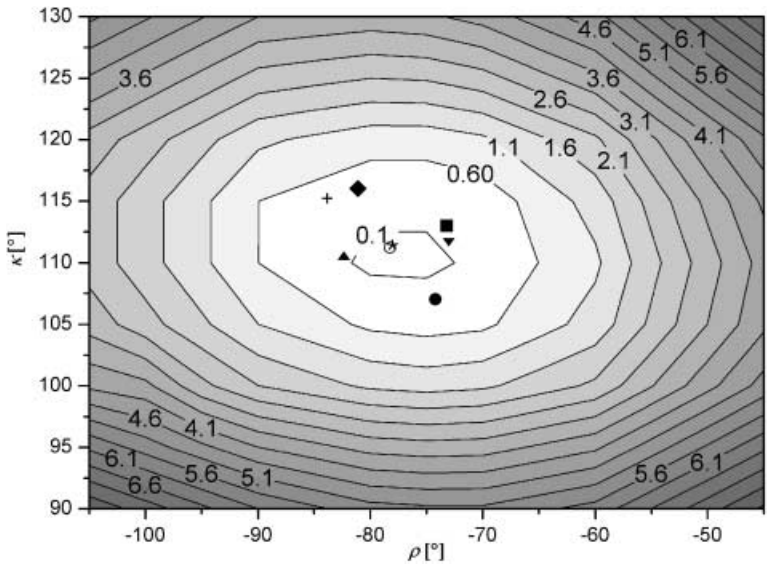


Figure 7. Energies [kcal mol$^{-1}$] of twisting, described by torsion angle $\rho$[N-Pd-C2$_a$-(2$_a$-H)], and tilting, described by torsion angle $\kappa$(Pd-C3$_a$-C1$_a$-C2$_a$) of the allyl group (minimum at $\rho = -77.0°$ and $\kappa = 111.2°$). Diphenylallyl complexes : ▲ (**2**; $-81.2°$, 109.6°); ● (**3**; $-73.9°$, 107.2°); + (**4a**; $-82.5°$, 114.3°); ○ (**4b**; $-77.1°$, 111.3°); ■ (*ent*-**5**; $-72.4°$, 112.2°). Dialkylallyl complexes of Part 1[55]: * (**6**; $-76.8°$, 111.3°); ▼ (**7**; $\kappa = -72.0°$, $\lambda = 111.0°$); ◆ (**8**; $-80.4°$, 115.6°).

## Discussion and Conclusion

Our results are relevant both for the understanding of the properties and equilibria of the ($\eta^3$-allyl)palladium complexes as well as their reactivities.

With regard to the ground state properties, our views expressed by Scheme 3 are fully supported by the isomer ratios observed for complexes with nonsymmetric allyl ligands. In particular, the allyl-bound phenyl group in complex **1** is a probe for assessing repulsive interactions of the PHOX ligand on the allylic moiety. This can be schematically expressed by the sector model shown in Figure 8. According

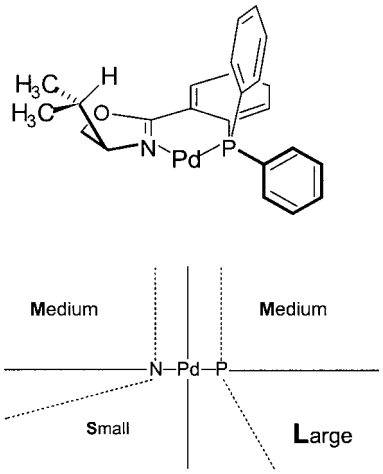


Figure 8. Sector model for PHOX ligands.

to this model, the dominant repulsive group of the PHOX ligand is the equatorial P-phenyl group. The classification of the lower left quadrant as being small is corroborated by complex **3** which displays a preference for the *exo*,*trans* isomer, wherein the plane of the phenyl group in the 3$_a$-*anti* position is perpendicularly arranged to the plane of the allyl ligand. Thus, the larger substituent, relative to the (PHOX)Pd moiety, at C3$_a$ occupies the lower left quadrant.

Complex **1** bears close resemblance to the reactive intermediate of the substitution, reported by Pfaltz et al.,[31] described in Scheme 6. This reaction mainly yields the linear product, nevertheless, the enantiomeric excess (*ee*) and configuration of the branched product were determined. The preferred branched product is the one that arises from the reaction of the most stable intermediate allyl complex, corresponding to **1xt**, at the allylic carbon *trans* to phosphorus. This was anticipated on the basis of the previous results with the thoroughly investigated 1,3-diphenyl-[8] or 1,3-dialkyl-allyl[5] derivatives.

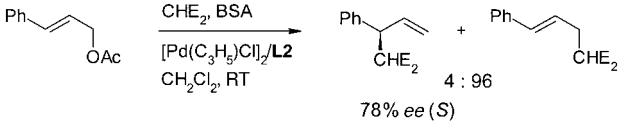


Scheme 6. Allylic substitution at a monosubstituted allyl acetate; E = $COOCH_3$, BSA = *N*,*O*-bis(trimethylsilyl)acetamide.

The structural characterization of complex **4** is particularly significant and provides very important new information on the catalytic cycle of the allylic substitution. Reactions of geminally disubstituted substrates (Scheme 7) are of interest

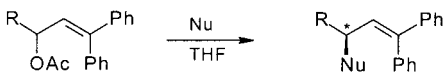


| R | Nu / conditions | Yield [%] | *ee* [%] |
|---|---|---|---|
| Me | $NaCH(COOMe)_2$ | 95 | 95 |
| Ph | 2.5 mol% $[\{Pd(C_3H_5)Cl\}_2]$ | 88 | 99 |
| | 10 mol% **L1** | | |
| Me | $BnNH_2$ (10 equiv) | 82 | 98 |
| *n*Bu | 5 mol% $[\{Pd(C_3H_5)Cl\}_2]$ | 30 | 94 |
| | 12 mol% **L4** | | |
| | 10 equiv AcOH, reflux | | |

Scheme 7. Allylic substitutions at trisubstituted allyl acetate.

as both electronic and steric effects guarantee a high degree of regioselectivity in favor of the chiral product. Substrates of this type were studied at an early stage,[32] good results (up to

  0947-6539/02/0814-3110 $ 17.50+.50/0 *Chem. Eur. J.* **2002**, *8*, No. 14

86% *ee*) had been obtained, even with chiraphos and sparteine[33] as chiral ligands. Standard phosphanyloxazolines, such as **L1**, induced superior enantioselectivity; however, the reactions were generally slow.[34] With the very bulky ligands **L4**[35] and **L5**,[36] in conjunction with appropriate leaving groups and reaction conditions, higher degrees of reactivity were achieved more recently.

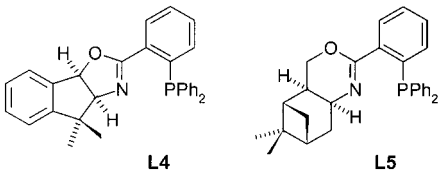


With the PHOX ligands **L1**–**L5** and substrates with a variety of substituents R, the steric course of the reaction was the same as that shown in Scheme 7. The remarkable point is that the preferred product in the case R = Ph can not arise from the *exo*,*trans* isomer (**4xt**) found in solution. Possible are reactions at the non-observed *endo*,*trans* (**4nt**) and *exo*,*cis* (**4xc**) isomers (cf. Scheme 8). If complex **4xt** does

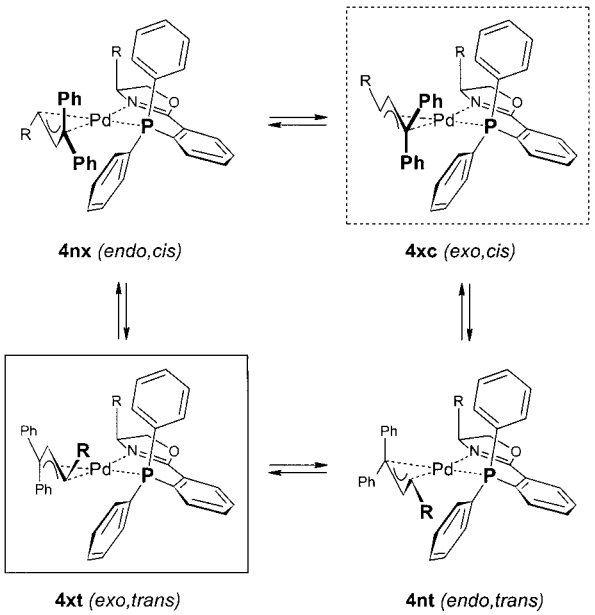


Scheme 8. The four possible *syn* isomers of complex **4**. Only isomer **4xt** was found in the crystal, isomer **4xc** is the most reactive in the substitution reaction.

not react at the allylic carbon *trans* to nitrogen, there is no reason to assume that complex **4nt** would do so. With this safe assumption, we can conclude that the reaction of the non-observed complex **4xc** at the carbon *trans* to P is faster by a factor of $>10000$ than the reaction of the observed complex **4xt** at the carbon *trans* to N. This value is derived from observed isomer ratios and enantioselectivities, both in the range $>100:1$. The isomer ratios of *trans* and *cis* allyl isomers is expected to be even higher with groups R that are smaller than phenyl. Given the generally high enantioselectivities, similar rate factors as in the reactions via complex **4** are to be expected.

This observation further substantiates the previous analysis for reactions involving *P*,*N* ligands which emphasize the preference of the attack at the C *trans* to P. The previous arguments relied on the fact that, in general, the Pd–$C3_a$ bond is longer and weaker than the Pd–$C1_a$ bond,[6b, 37] the observation of a product olefin complex,[8] and inertness to addition of a nucleophile for $\eta^3$-allyl complexes with very strong steric shielding in the vicinity of $C3_a$.[7]

The low overall reaction rates obtained with complexes **L1**–**L3** are understandable considering the low concentration of the reactive isomer. In addition, interconversion rates among allyl isomers shown in Scheme 8 are probably low because the route from **4xt** to **4xc** must involve formation of a $\eta^1$-allyl complex with a bond between Pd and the tertiary carbon or a ligand dissociation process. The higher rates achieved with the bulky ligands **L4** and **L5** could be the result of an enhanced population of the *exo*,*cis*-isomers or ground state destabilization.

## Experimental Section

Ligands were synthesized as previously described.[38] The complexes were prepared under dry argon using standard Schlenk techniques. $^1$H, $^{13}$C, and $^{31}$P NMR spectra were recorded on Bruker AMX400, DRX500 or DMX600 instruments. $^1$H NMR chemical shifts are relative to residual undeuterated solvent in $CDCl_3$ ($\delta = 7.26$), the $^{13}$C NMR shifts are relative to the solvent $CDCl_3$ ($\delta = 77.0$), and the $^{31}$P NMR shifts are relative to 85% $H_3PO_4$ ($\delta = 0.00$). NOESY spectra were recorded with a mixing time of 100, 200, 300 or 600 ms, TOCSY spectra were recorded with a mixing time of 60 ms. Melting points were determined in open glass capillaries and are not corrected. Optical rotations were measured on a Perkin Elmer 241 MC polarimeter. Crystallographic data were collected on a three-circle diffractometer (Bruker Smart CCD) with a CCD detector. Intensities were corrected for Lorentzian and polarization effects. An empirical absorption correction was applied with the SADABS program[39] based on the Laue symmetry of the reciprocal space. The structures were solved by direct methods and refined against $F^2$ with a full-matrix least-squares algorithm with the SHELXTL-PLUS (5.03) software package.[40]

**General procedure for preparation of ($\eta^3$-allyl)(PHOX)palladium complexes**: A solution of silver salt (0.513 mmol) in methanol (2 mL) was added to a solution of the PHOX ligand (0.525 mmol) and [{($\eta^3$-(phenyl)-allyl)PdCl}$_2$] (0.250 mmol) in $CH_2Cl_2$ (5 mL). After stirring for 1 h in the dark, the solution was filtered through celite, the residue washed with $CH_2Cl_2$, and the filtrate concentrated in vacuo. Single crystals suitable for X-ray measurement were grown either by slow evaporation of a diluted solution of the crude product or by employing the following diffusion method: the crude product was dissolved in $CH_2Cl_2$ (2–3 mL), the solution transferred into a test-tube which was placed into a wide-necked bottle containing a 1-cm layer of diethyl ether or hexane. The tightly closed bottle was then stored in a refrigerator at $-4\,^\circ$C or $-20\,^\circ$C. Crystals usually appeared after a few days.

**($\eta^3$-1-Phenylallyl)-{(4*S*)-[2-(2′-diphenylphosphanyl)phenyl]-4,5-dihydro-4-(2-propyl)oxazole}palladium(II) hexafluoroantimonate (1)**: This compound was prepared according to the general procedure from [{($\eta^3$-1-phenylallyl)PdCl}$_2$] (258.5 mg, 0.500 mmol), **L1** (392.0 mg, 1.050 mmol), and $AgSbF_6$ (352.0 mg, 1.025 mmol). Single crystals were grown by the evaporation method from $CH_2Cl_2$/hexane/*tert*-butyl methyl ether at room temperature. Yield of **1**: 640.0 mg (77%), light yellow crystals; m.p. $>250\,^\circ$C; $[\alpha]_D^{20} = +237.3$ ($c = 2.44$, $CH_2Cl_2$).

**1xt (*exo*,*trans*)**: 57.5%; $^1$H NMR (600.13 MHz, $CD_2Cl_2$, $-20\,^\circ$C): $\delta = -0.18$ (d, $^3J(1_s\text{-H},2_s\text{-H}) = 6.8$ Hz, 3H; $2_s$-H), 0.13 (d, $^3J(1_s\text{-H},3_s\text{-H}) = 6.8$ Hz, 3H; $3_s$-H), 1.30 (dqq, $^3J(4\text{-H},1_s\text{-H}) = 3.5$ Hz, $^3J(1_s\text{-H},2_s\text{-H}) = 6.8$ Hz, $^3J(2_s\text{-H},3_s\text{-H}) = 6.8$ Hz, 1H; $1_s$-H), 2.77 (d, $^3J(1_a\text{-H}_{anti},2_a\text{-H}) = 11.7$ Hz, 1H; $1_a\text{-H}_{anti}$), 3.35 (ddd, $^3J(4\text{-H},1_s\text{-H}) = 3.6$ Hz, $^3J(4\text{-H},5\text{-H}_{Re}) = 5.3$ Hz, $^3J(4\text{-H},5\text{-H}_{Si}) = 9.5$ Hz, 1H; 4-H), 3.48 (dd, $^2J(1_a\text{-H}_{syn},1_a\text{-H}_{anti}) \approx 2.5$ Hz, $^3J(1_a\text{-H}_{syn},2_a\text{-H}) =$

7.1 Hz, 1H; $1_a$-$H_{syn}$), 4.10 (dd, $^3J$(4-H,5-$H_{Re}$) = 5.3 Hz, $^2J$(5-$H_{Re}$,5-$H_{Si}$) = 9.5 Hz, 1H; 5-$H_{Re}$), 4.20 (dd, $^2J$(5-$H_{Si}$,5-$H_{Re}$) = 9.5 Hz, $^3J$(4-H,5-$H_{Si}$) ≈ 9.5 Hz, 1H; 5-$H_{Si}$), 5.58 (dd, $^3J$($3_a$-H,P) = 9.9 Hz, $^3J$($2_a$-H,$3_a$-H) = 13.8 Hz, 1H; $3_a$-H), 6.37 (ddd, $^3J$($1_a$-$H_{syn}$,$2_a$-H) = 7.1 Hz, $^3J$($1_a$-$H_{anti}$,$2_a$-H) = 11.7 Hz, $^3J$($2_a$-H,$3_a$-H) = 13.8 Hz, 1H; $2_a$-H), 7.10 (dd, $^3J$(8-H,9-H) ≈ 8 Hz, $^3J$(8-H,P) ≈ 10 Hz, 1H; 8-H), 7.39 (m, 2H; $5_a$-H), ≈7.5 (m, 3H; $6_a$-H, $7_a$-H), 7.60 (m, 1H; 9-H), 7.70 (dddd, $^5J$(10-H,P) ≈ 1 Hz, $^4J$(8-H,10-H) ≈ 1 Hz, $^3J$(9-H,10-H) ≈ 7.8 Hz, $^3J$(10-H,11-H) ≈ 7.8 Hz, 1H; 10-H), 8.20 (ddd, $^4J$(9-H,11-H) ≈ 1.1 Hz, $^4J$(11-H,P) = 4.4 Hz, $^3J$(10-H,11-H) = 7.7 Hz, 1H; 11-H); $^{13}$C NMR (125.76 MHz, $CD_2Cl_2$, −20 °C): δ = 12.27 ($C2_s$), 17.69 ($C3_s$), 30.66 ($C1_s$), 51.60 ($C1_a$), 68.22 (C5), 69.95 (C4), 101.47 ($C3_a$), 113.22 ($C2_a$), ca. 128.2 (C6), ca. 28.9 (C7), ca. 129.60 ($C6_a$, $C7_a$), ca. 132.00 (C9), 132.17 (C10), ca. 133.2 (C11), 134.10 ($C5_a$), 134.80 (C8), 135.67 ($C4_a$), ca. 164 (C2); $^{31}$P NMR (202.46 MHz, $CD_2Cl_2$, −20 °C): δ = 24.29.

***1nt (endo,trans)***: 38%; $^1$H NMR: δ = 0.14 (d, $^3J$($1_s$-H,$2_s$-H) = 6.8 Hz, 3H; $2_s$-H), 0.65 (d, $^3J$($1_s$-H,$3_s$-H) = 6.8 Hz, 3H; $3_s$-H), 1.93 (dqq, $^3J$(4-H,$1_s$-H) = 3.6 Hz, $^3J$($1_s$-H,$2_s$-H) = 6.8 Hz, $^3J$($1_s$-H,$3_s$-H) = 6.8 Hz, 1H; $1_s$-H), 3.21 (d, $^3J$($1_a$-$H_{anti}$,$2_a$-H) ≈ 12 Hz, 1H; $1_a$-$H_{anti}$), 3.24 (dd, $^2J$($1_a$-$H_{anti}$,$1_a$-$H_{syn}$) ≈ 2 Hz, $^3J$($1_a$-$H_{syn}$,$2_a$-H) ≈ 7 Hz, 1H; $1_a$-$H_{syn}$), 3.31 (m, 1H; 4-H), 4.00 (dd, $^2J$(5-$H_{Re}$,5-$H_{Si}$) = 9.6 Hz, $^3J$(4-H,5-$H_{Si}$) = 9.6 Hz, 1H; 5-$H_{Re}$), 4.16 (dd, $^3J$(4-H,5-$H_{Re}$) = 5.6 Hz, $^2J$(5-$H_{Re}$,5-$H_{Si}$) = 9.6 Hz, 1H; 5-$H_{Si}$), 5.34 (dd, $^3J$($3_a$-H,P) = 11 Hz, $^3J$($2_a$-H,$3_a$-H) = 12 Hz, 1H; $3_a$-H), 6.26 (ddd, $^3J$($1_a$-$H_{syn}$,$2_a$-H) = 7 Hz, $^3J$($1_a$-$H_{anti}$,$2_a$-H) = 12 Hz, $^3J$($2_a$-H,$3_a$-H) = 12 Hz, 1H; $2_a$-H), 7.07 (dd, $^3J$(8-H,9-H) = 7.8 Hz, $^3J$(8-H,P) ≈ 10 Hz, 1H; 8-H), 7.35 (m, 2H; $5_a$-H), 7.45 (m, 2H; $6_a$-H), 7.59 (m, 1H; 9-H), 7.65 (m, 1H; $7_a$-H), 7.67 (dddd, $^5J$(10-H,P) ≈ 1 Hz, $^4J$(8-H,10-H) ≈ 1 Hz, $^3J$(9-H,10-H) ≈ 7.8 Hz, $^3J$(10-H,11-H) ≈ 7.8 Hz, 1H; 10-H), 8.16 (ddd, $^4J$(9-H,11-H) ≈ 1.1 Hz, $^4J$(11-H,P) = 4.4 Hz, $^3J$(10-H,11-H) = 7.7 Hz, 1H; 11-H); $^{13}$C NMR: δ = 13.04 ($C2_s$), 17.88 ($C3_s$), 31.47 ($C1_s$), 55.80 ($C1_a$), 68.22 (C5), 69.95 (C4), 98.50 ($C3_a$), 115.31 ($C2_a$), 127.40 ($C7_a$), ca. 128.20 (C6), ca. 128.90 (C7), 129.50 ($C6_a$), ca. 132.00 (C9, C10), ca. 133.20 (C11), 134.05 ($C5_a$), 134.95 (C8), 136.18 ($C4_a$), ca. 164 (C2); $^{31}$P NMR: δ = 22.90.

***1xc (exo,cis)***: 3.5%; $^1$H NMR: δ = 0.36 (d, $^3J$($1_s$-H,$2_s$-H) = 6.8 Hz, 3H; $2_s$-H), 0.84 (d, $^3J$($1_s$-H,$3_s$-H) = 6.8 Hz, 3H; $3_s$-H), 2.07 (dqq, $^3J$(4-H,$1_s$-H) = 3.3 Hz, $^3J$($1_s$-H,$2_s$-H) = 6.9 Hz, $^3J$($1_s$-H,$3_s$-H) = 6.9 Hz, 1H; $1_s$-H), 4.03 (dd, $^3J$($2_a$-H,$3_a$-$H_{anti}$) ≈ 10 Hz, $^3J$($3_a$-$H_{anti}$,P) ≈ 10 Hz, 1H; $3_a$-$H_{anti}$), 4.32 (d, $^3J$($1_a$-H,$2_a$-H) = 11.8 Hz, 1H; $1_a$-H), 4.37 (m, 1H; 5-$H_{Re}$), 4.42 (m, 1H; 4-H), 4.62 (dd, $^3J$(4-H,5-$H_{Si}$) = ≈ 9 Hz, $^2J$(5-$H_{Si}$,5-$H_{Re}$) ≈ 9Hz, 1H; 5-$H_{Si}$), 4.91 (dd, $^3J$($3_a$-$H_{syn}$,P) = 6 Hz, $^3J$($2_a$-H,$3_a$-$H_{syn}$) = 7.3 Hz, 1H; $3_a$-$H_{syn}$), 6.46 (ddd, $^3J$($2_a$-H,$3_a$-$H_{syn}$) ≈ 7 Hz, $^3J$($2_a$-H,$3_a$-$H_{anti}$) ≈ 12 Hz, $^3J$($2_a$-H,$3_a$-H) ≈ 12 Hz, 1H; $2_a$-H), ≈7.10 (m, 1H; 8-H), ≈7.60 (m, 1H; 9-H), 7.68 (m, 1H; 10-H), 8.24 (ddd, $^4J$(9-H,11-H) ≈ 1.1 Hz, $^4J$(11-H,P) = 4.4 Hz, $^3J$(10-H,11-H) = 7.7 Hz, 1H; 11-H); $^{13}$C NMR: δ = 14.22 ($C2_s$), 17.84 ($C3_s$), ca. 31.00 ($C1_s$), 68.79 (C5), 75.00 ($C1_a$), 77.34 (C4), 78.31 ($C3_a$) 119.66 ($C2_a$), 133.10 (C11), ca. 164 (C2); $^{31}$P NMR: δ = 19.83.

***1nc (endo,cis)***: 1%; $^1$H NMR: δ = 0.19 (d, $^3J$($1_s$-H,$2_s$-H) = 6.8 Hz, 3H; $2_s$-H), 0.91 (d, $^3J$($1_s$-H,$3_s$-H) = 6.8 Hz, 3H; $3_s$-H), 2.10 (m, 1H; $1_s$-H), 3.91 (dd, $^3J$($3_a$-$H_{anti}$,P) = 10.8 Hz, $^3J$($2_a$-H,$3_a$-$H_{anti}$) = 13.4 Hz, 1H; $3_a$-$H_{anti}$), 4.42 (m, 1H; 4-H), 4.75 (dd, $^3J$($2_a$-H,$3_a$-$H_{syn}$) = 7.3 Hz, $^3J$($3_a$-$H_{syn}$,P) = 7.5 Hz, 1H; $3_a$-$H_{syn}$), 4.83 (d, $^3J$($1_a$-H,$2_a$-H) = 12 Hz, 1H; $1_a$-H), 6.31 (ddd, $^3J$($2_a$-H,$3_a$-$H_{syn}$) ≈ 7 Hz, $^3J$($2_a$-H,$3_a$-$H_{anti}$) ≈ 12 Hz, $^3J$($1_a$-H,$2_a$-H) ≈ 12 Hz, 1H; $2_a$-H); $^{13}$C NMR: δ = ca. 13.00 ($C2_s$), 18.19 ($C3_s$), 74.04 ($C3_a$), 77.45 ($C1_a$), ca. 115.00 ($C2_a$), ca. 164 (C2); $^{31}$P NMR: δ = 23.79.

Elemental analysis (%) calcd for $C_{33}H_{33}F_6NOPPdSb$ (832.76): C 47.59, H 3.99, N 1.68, P 3.72; found: C 47.52, H 4.00, N 1.63, P 3.80.

**($\eta^3$-1,3-Diphenylallyl)-{(4*S*)-[2-(2′-diphenylphosphanyl)phenyl]-4,5-dihydro-4-(2-propyl)oxazole}palladium(II) hexafluoroantimonate (2)**: This compound was prepared according to the general procedure from [{($\eta^3$-1,3-diphenylallyl)PdCl}$_2$] (105.4 mg, 0.157 mmol), **L1** (129.2 mg, 0.346 mmol), and $AgSbF_6$ (108.1 mg, 0.315 mmol). Crystals were grown by the evaporation method from $CH_2Cl_2$/ethyl acetate at room temperature. Yield of **2**: 151.0 mg (88%); m.p. 239–241 °C; $[\alpha]_D^{20}$ = +374.6 (*c* = 2.48, $CH_2Cl_2$).

***exo***: 89%; $^1$H NMR (300.13 MHz, $CDCl_3$, 20 °C): δ = −0.06 (d, $^3J$($1_s$-H,$2_s$-H) = 6.7 Hz, 3H; $2_s$-H), 0.27 (d, $^3J$($1_s$-H,$3_s$-H) = 6.9 Hz, 3H; $3_s$-H), 1.59 (m, 1H; $1_s$-H), 3.12 (ddd, $^3J$(4-H,$1_s$-H) = 3.5 Hz, $^3J$(4-H,5-$H_{Re}$) = 4.9 Hz, $^3J$(4-H,5-$H_{Si}$) = 9.5 Hz, 1H; 4-H), 4.00–4.12 (m, $^3J$(4-H,5-$H_{Re}$) = 5.1 Hz, $^3J$(4-H,5-$H_{Si}$) = 9.1 Hz, $^2J$(5-$H_{Re}$,5-$H_{Si}$) = 9.1 Hz, 2H; 5-$H_{Re}$, 5-$H_{Si}$), 4.28 (d, $^1J$($1_a$-H,$2_a$-H) = 11.0 Hz, 1H; $1_a$-H), 5.84 (dd, $^3J$($3_a$-H,P) = 9.4 Hz, $^3J$($2_a$-H,$3_a$-H) = 13.8 Hz, 1H; $3_a$-H), 6.82 (dd, $^3J$($1_a$-H,$2_a$-H) = 11.1 Hz, $^3J$($2_a$-H,$3_a$-H) = 13.8 Hz, 1H; $2_a$-H), 6.87–7.10 (m, 10H; Ar-H), 7.28–7.66 (m, 11H; Ar-H), 7.81 (m, 2H; Ar-H), 8.12 (ddd, $^4J$(8-H,11-H) = 1.0 Hz, $^4J$(11-H,P) = 4.0 Hz, $^3J$(10-H,11-H) = 7.0 Hz, 1H; 11-H); $^{13}$C NMR (75.47 MHz, $CDCl_3$, 20 °C): δ = 13.26 ($C3_s$), 18.01 ($C2_s$), 30.88 ($C1_s$), 68.09 (C5), 69.33 (C4), 70.87 ($C1_a$), 100.24 (d, $^2J_{3,P}$ = 23 Hz, $C3_a$), 111.56 ($C2_a$), 127.06, 127.10, 128.51, 129.10, 129,24, 129.36, 129.51, 129.98, 130.98, 132.01, 132.50, 132.67, 133.01, 133.09, 133.17, 133.28, 133.80, 133.98, 135.24 (d, Ar-C), 127.22, 127.94, 129.65, 135.88, 135.96 (s, Ar-C), 164.16 (C2); $^{31}$P NMR (81.02 MHz, [$D_8$]THF, 20 °C): δ = 22.67.

***endo***: 11%; $^1$H NMR (300.13 MHz, $CDCl_3$, 20 °C): δ = −0.06 (d, $^3J$($1_s$-H,$2_s$-H) = 6.7 Hz, 3H; $2_s$-H), 0.76 (d, $^3J$($1_s$-H,$3_s$-H) = 6.9 Hz, 3H; $3_s$-H), 2.09 (m, 1H; $1_s$-H), 3.40 (m, 1H; 4-H), 5.10 (d, $^3J$($1_a$-H,$2_a$-H) = 12.0 Hz, 1H; $1_a$-H), 5.68 (dd, $^3J$($3_a$-H,P) = 11.0 Hz, $^3J$($2_a$-H,$3_a$-H) = 11.0 Hz, 1H; $3_a$-H), 6.50 (dd, $^3J$($1_a$-H,$2_a$-H) = 12.0 Hz, $^3J$($2_a$-H,$3_a$-H) = 12.0 Hz, 1H; $2_a$-H), 8.06 (ddd, $^4J$(8-H,11-H) = 1.0 Hz, $^4J$(11-H,P) = 4.0 Hz, $^3J$(10-H,11-H) = 7.0 Hz, 1H; 11-H); $^{31}$P NMR (81.02 MHz, [$D_8$]THF, 20 °C): δ = 26.94.

Elemental analysis (%) calcd for $C_{39}H_{37}F_6NOPPdSb$ (908.8): C 51.54, H 4.10, P 3.41; found: C 51.49, H 4.30, P 3.47.

**($\eta^3$-1,1-Diphenylallyl)-{(4*S*)-[2-(2′-diphenylphosphanyl)phenyl]-4,5-dihydro-4-(2-propyl)oxazole}palladium(II) perchlorate (3)**: This compound was prepared according to the general procedure from [{($\eta^3$-1,1-diphenylallyl)PdCl}$_2$] (86.5 mg, 0.129 mmol), **L1** (101.0 mg, 0.269 mmol), and $AgClO_4$ (55.1 mg, 0.266 mmol). Crystals were grown by the diffusion method from $CH_2Cl_2$/diethyl ether at −4 °C. Yield of **3**: 159.0 mg (80%); m.p. 248–250 °C; $[\alpha]_D^{24}$ = +81.8 (*c* = 1.08, $CHCl_3$); $^1$H NMR (500.13 MHz, $CDCl_3$, 20 °C): δ = −0.10 (d, $^3J$($1_s$-H,$2_s$-H) = 7.3 Hz, 3H; $2_s$-H), 0.43 (d, $^3J$($1_s$-H,$3_s$-H) = 6.9 Hz, 3H; $3_s$-H), 1.77 (dqq, $^3J$(4-H,$1_s$-H) = 2.9 Hz, $^3J$($1_s$-H,$2_s$-H) = 6.7 Hz, $^3J$($1_s$-H,$3_s$-H) = 6.7 Hz, 1H; $1_s$-H), 2.62 (br s, 1H; $1_a$-$H_{anti}$), 3.44 (br s, 1H; $1_a$-$H_{syn}$), 3.71 (br s, 1H; 4-H), 4.24 (dd, $^3J$(4-H,5-$H_{Re}$) = 4.6 Hz, $^2J$(5-$H_{Re}$,5-$H_{Si}$) = 9.4 Hz, 1H; 5-$H_{Re}$), 4.36 (dd, $^3J$(4-H,5-$H_{Si}$) = 9.7 Hz, $^3J$(5-$H_{Re}$,5-$H_{Si}$) = 9.7 Hz, 1H; 5-$H_{Si}$), 6.68 (dd, $^3J$($1_a$-$H_{syn}$,$2_a$-H) = 8.1 Hz, $^3J$($1_a$-$H_{anti}$,$2_a$-H) = 11.7 Hz, 1H; $2_a$-H), 6.88 (dd, $^3J$($2_{Si}$-H,$3_{Si}$-H) = 7.6 Hz, $^3J$($2_{Si}$-H,P) = 12.6 Hz, 2H; $2_{Si}$-H), 7.00 (ddd, $^4J$(8-H,10-H) = 1.2 Hz, $^3J$(8-H,9-H) = 7.6 Hz, $^3J$(8-H,P) = 9.0 Hz, 1H; 8-H), 7.15 (m, 2H; $9_a$-H), 7.34 (m, 3H; $3_{Si}$-H, $11_a$-H), 7.36 (m, 4H; $2_{Re}$-H, $10_a$-H), 7.45 (dt, $^4J$($2_{Si}$-H,$4_{Si}$-H) = 1.7 Hz, $^3J$($3_{Si}$-H,$4_{Si}$-H) = 7.3 Hz, m, 1H; $4_{Si}$-H), 7.47 (m, 2H; $6_a$-H), 7.52 (m, 2H; $3_{Re}$-H), 7.56 (m, 1H; 9-H), 7.58 (m, 2H; $5_a$-H), 7.60 (m, 1H; $4_{Re}$-H), 7.68 (m, 1H; $7_a$-H), 7.69 (dd, $^3J$(9-H,10-H) = 7.8 Hz, $^3J$(10-H,11-H) = 7.8 Hz, 1H; 10-H), 8.24 (ddd, $^4J$(8-H,11-H) = 1.1 Hz, $^4J$(11-H,P) = 4.4 Hz, $^3J$(10-H,11-H) = 8.1 Hz, 1H; 11-H); $^{13}$C NMR (125.76 MHz, $CDCl_3$, 20 °C): δ = 12.37 ($C3_s$), 18.09 ($C2_s$), 30.45 ($C1_s$), 50.88 ($C1_a$), 67.93 (C5), 70.27 (C4), 113.24 ($C2_a$), 127.26 ($C4_{Re}$), 127.99 ($C2_{Re}$), 128.37 (C6), 128.76 (C7), 129.14 ($C9_a$), 129.72 ($C3_{Re}$), 131.39 ($C4_{Si}$), 132.18 ($C2_{Si}$), 132.24 (C10), 132.48 ($C5_a$), 133.29 (C9), 133.51 (C11), 133.70 ($C7_a$), 134.57 (C8), 135.92 ($C8_a$), 138.85 ($C4_a$), 164.27 (C2); $^{31}$P NMR (202.46 MHz, $CDCl_3$, 20 °C): δ = 26.61; elemental analysis (%) calcd for $C_{39}H_{37}ClNO_5PPd$ (772.57): C 60.63, H 4.83, N 1.81; found: C 60.24, H 5.11, N 1.85.

**($\eta^3$-1,1,3-Triphenylallyl)-{(4*S*)-[2-(2′-diphenylphosphanyl)phenyl]-4,5-dihydro-4-(2-propyl)oxazole}palladium(II) hexafluoroantimonate (4)**: This compound was prepared according to the general procedure from [{($\eta^3$-1,1,3-triphenylallyl)PdCl}$_2$] (206.0 mg, 0.250 mmol), **L1** (196.0 mg, 0.525 mmol), and $AgSbF_6$ (175.0 mg, 0.510 mmol). Crystals were grown by the diffusion method from $CH_2Cl_2$/hexane at −20 °C. Yield of **4**: 443.0 mg (90%), light brown crystals; m.p. 145–147 °C; $[\alpha]_D^{20}$ = +251.7 (*c* = 1.07, $CHCl_3$); $^1$H NMR (600.13 MHz, $CDCl_3$, 27 °C): δ = 0.08 (d, $^3J$($1_s$-H,$2_s$-H) = 6.8 Hz, 3H; $2_s$-H), 0.67 (d, $^3J$($1_s$-H,$3_s$-H) = 6.8 Hz, 3H; $3_s$-H), 2.17 (dqq, $^3J$(4-H,$1_s$-H) = 3.2 Hz, $^3J$($1_s$-H,$2_s$-H) = 6.8 Hz, $^3J$($1_s$-H,$3_s$-H) = 6.8 Hz, 1H; $1_s$-H), 3.62 (ddd, $^3J$(4-H,$1_s$-H) = 3.2 Hz, $^3J$(4-H,5-$H_{Re}$) = 5 Hz, $^3J$(4-H,5-$H_{Si}$) = 10 Hz, 1H; 4-H), 4.10 (d, $^3J$($1_a$-H,$2_a$-H) = 11.5 Hz, 1H; $1_a$-H), 4.33 (dd, $^3J$(4-H,5-$H_{Re}$) = 5 Hz, $^2J$(5-$H_{Re}$,5-$H_{Si}$) = 9.6 Hz, 1H; 5-$H_{Re}$), 4.37 (dd, $^3J$(4-H,5-$H_{Si}$) ≈ 9 Hz, $^2J$(5-$H_{Si}$,5-$H_{Re}$) = 9.6 Hz, 1H; 5-$H_{Si}$), 6.52 (dd, $^3J$($2_{Si}$-H,$3_{Si}$-H) = 7.9 Hz, $^3J$($2_{Si}$-H,P) = 12.4 Hz, 2H; $2_{Si}$-H), 6.76 (dd, $^3J$($2_{Re}$-H,$3_{Re}$-H) = 7.9 Hz, $^3J$($2_{Re}$-H,P) = 12.4 Hz, 2H; $2_{Re}$-H), 6.92 (d, $^3J$($13_a$-H,$14_a$-H) = 7.7 Hz, 2H; $13_a$-H), 7.04 (dd, $^3J$($13_a$-H,$14_a$-H) = 7.7 Hz, $^3J$($14_a$-H,$15_a$-H) = 7.7 Hz, 2H; $14_a$-H), 7.04 (ddd, $^4J$(8-H,10-H) = 1.1 Hz, $^3J$(8-H,P) = 7 Hz, $^3J$(8-H,9-H) = 7.7 Hz, 1H; 8-H), 7.13 (tt, $^4J$($13_a$-H,$15_a$-H) = 1.1 Hz, $^3J$($14_a$-H,$15_a$-H) = 7.7 Hz, 1H; $15_a$-H), 7.20 (d, $^3J$($1_a$-H,$2_a$-H) = 11.5 Hz, 1H; $2_a$-H), 7.30 (m, 2H; $3_{Re}$-H), 7.31 (m, 2H; $3_{Si}$-H), 7.37 (m, 2H; $9_a$-H), 7.41 (m, 3H; $10_a$-H, $11_a$-H), 7.42 (m, 1H; $4_{Re}$-H), 7.47 (m, 3H; $6_a$-H, $7_a$-H), 7.53 (t, $^3J$($3_{Si}$-H,$4_{Si}$-H) = 7.7 Hz, 1H; $4_{Si}$-H), 7.58 (dd, $^3J$(8-H,9-H) = 7.7 Hz, $^3J$(9-H,10-H) = 7.7 Hz, 1H; 9-H), 7.74 (dddd, $^5J$(10-H,P) =



0947-6539/02/0814-3112 $ 17.50+.50/0 *Chem. Eur. J.* **2002**, *8*, No. 14

1.1 Hz, $^4J$(8-H,10-H) = 1.1 Hz, $^3J$(9-H,10-H) = 7.7 Hz, $^3J$(10-H,11-H) = 7.7 Hz, 1H; 10-H), 7.89 (m, 2H; $5_a$-H), 8.26 (ddd, $^4J$(9-H,11-H) = 1.1 Hz, $^4J$(11-H,P) = 4.4 Hz, $^3J$(10-H,11-H) = 7.7 Hz, 1H; 11-H); $^{13}$C NMR (125.76 MHz, $CDCl_3$, 27 °C): $\delta$ = 11.67 ($C3_s$), 16.56 ($C2_s$), 30.10 ($C1_s$), 67.15 (C5), 68.67 (C4), 70.09 ($C1_a$), 108.14 ($C2_a$), 118.10 ($C3_a$), 125.00 ($C1_{Re}$), 125.55 ($C1_{Si}$), 126.10 ($C13_a$), 126.31 ($C15_a$), 126.90 ($C5_a$), 127.57 ($C14_a$), 127.85 ($C4_{Re}$), 127.87 (C6), 128.00 ($C3_{Re}$), 128.05 ($C3_{Si}$), 128.38 (C7), 128.50 ($C6_a$, $C7_a$), 128.80 ($C10_a$), 128.95 ($C9_a$), 130.10 ($C4_{Si}$), 131.00 ($C11_a$), 131.24 (C10), 131.81 ($C2_{Si}$), 132.14 (C11), 132.36 (C9), 132.73 ($C2_{Re}$), 135.55 ($C8_a$), 136.62 (C8), 136.78 ($C12_a$), 137.77 ($C4_a$), 163.60 (C2); $^{31}$P NMR (202.46 MHz, $CDCl_3$, 27 °C): $\delta$ = 21.81; elemental analysis (%) calcd for $C_{45}H_{41}F_6NOPPdSb$ (984.95): C 54.88, H 4.20, N 1.42, P 3.14; found: C 54.83, H 4.27, N 1.38, P 3.39.

## Acknowledgements

This work was supported by the Deutsche Forschungsgemeinschaft and the Fonds der Chemischen Industrie. We thank Dr. Quin Zhu-Ohlbach for preliminary semiempirial quantum-chemical calculations and Prof. M. Reggelin, Darmstadt, for helpful discussions. Furthermore, we thank one of the referees for helpful comments on the crystal structure of complex **1** which led to an improvement of the structure.

[1] Recent reviews: a) B. M. Trost, C. Lee in *Catalytic Asymmetric Synthesis*, 2nd ed.; (Ed.: I. Ojima), Wiley-VCH, New York, **2000**, pp. 593–649; b) A. Pfaltz, M. Lautens in *Comprehensive Asymmetric Catalysis*, (Eds.: E. N. Jacobsen, A. Pfaltz, H. Yamamoto), Springer, Heidelberg, **1999**, pp. 833–886; c) B. M. Trost, D. L. Van Vranken, *Chem. Rev.* **1996**, *96*, 395–422.

[2] a) J. Sprinz, G. Helmchen, *Tetrahedron Lett.* **1993**, *34*, 1769–1772; b) P. von Matt, A. Pfaltz, *Angew. Chem.* **1993**, *105*, 614–615; *Angew. Chem. Int. Ed. Engl.* **1993**, *32*, 566–568; c) G. J. Dawson, C. G. Frost, J. M. J. Williams, S. J. Coote, *Tetrahedron Lett.* **1993**, *34*, 3149–3150; d) G. Helmchen, A. Pfaltz, *Acc. Chem. Res.* **2000**, *33*, 336–345.

[3] B. M. Trost, *Acc. Chem. Res.* **1996**, *32*, 566–568, and literature therein.

[4] G. Knühl, P. Sennhenn, G. Helmchen, *J. Chem. Soc. Chem. Commun* **1995**, 1845–1846.

[5] M. Kollmar, B. Goldfuss, M. Reggelin, F. Rominger, G. Helmchen, *Chem. Eur. J.* **2001**, *7*, 4913–4927.

[6] a) G. Helmchen, S. Kudis, P. Sennhenn, H. Steinhagen, *Pure Appl. Chem.* **1997**, *69*, 513–518; b) J. Sprinz, M. Kiefer, G. Helmchen, M. Reggelin, G. Huttner, O. Walter, L. Zsolnai, *Tetrahedron Lett.* **1994**, *35*, 1523–1526.

[7] A. Togni, U. Burckhardt, V. Gramlich, P. S. Pregosin, R. Salzmann, *J. Am. Chem. Soc.* **1996**, *118*, 1031–1037.

[8] a) H. Steinhagen, M. Reggelin, G. Helmchen, *Angew. Chem.* **1997**, *109*, 2199–2202; *Angew. Chem. Int. Ed. Engl.* **1997**, *36*, 2108–2110; b) J. Junker, B. Reif, H. Steinhagen, B. Junker, I. C. Felli, M. Reggelin, Ch. Griesinger, *Chem. Eur. J.* **2000**, *6*, 3281–3286.

[9] For a recent review on computational aspects of [(allyl)Pd] complexes, see: a) A. Didieu, *Chem. Rev.* **2000**, *100*, 543–600; see also: b) H. Fujimoto, S. Tomohiro, *Int. J. Quant. Chem.* **1999**, *74*, 735–744.

[10] a) J. M. Brown, D. I. Hulmes, P. J. Guiry, *Tetrahedron* **1994**, 4493–4506; b) T. D. W. Claridge, J. M. Long, J. M. Brown, D. Hibbs, M. B. Hursthouse, *Tetrahedron* **1997**, *53*, 4035–4050; c) D. A. Evans, K. R. Campos, J. S. Tedrow, F. E. Michael, M. R. Gagne, *J. Am. Chem. Soc.* **2000**, *122*, 7905–7920.

[11] The full set of the possible reactions is described in Scheme 12.14 of G. Helmchen, H. Steinhagen, S. Kudis in *Transition Metal Catalysed Reactions* (Eds.: S.-I. Murahashi, S. G. Davies), Blackwell Science, Oxford, **1999**, pp. 241–260.

[12] P. R. Auburn, P. B. Mackenzie, B. Bosnich, *J. Am. Chem. Soc.* **1985**, *107*, 2033–2046.

[13] The numbering of atoms is identical to that in ref. 12 of Part 1. This is also valid for complexes **1**, **3** and **4** with an unsymmetrical allyl group.

[14] H. Steinhagen, Dissertation, Heidelberg, **1998**.

[15] CCDC-165698 (**1**), CCDC-169914 (**2**), CCDC-165699 (**3**), CCDC-165700 (**4**), and CCDC-165701 (**5**) contain the supplementary crystallographic data for this paper. These data can be obtained free of charge via www.ccdc.cam.ac.uk/conts/retrieving.html (or from the Cambridge Crystallographic Data Centre, 12 Union Road, Cambridge CB2 1EZ, UK; fax: (+44) 1223-336033; or deposit@ccdc.cam.uk).

[16] A. G. Orpen, L. Brammer, F. H. Allen, O. Kennard, D. B. Watson, R. Tyler, *J. Chem. Soc. Dalton Trans.* **1989**, S1-S83.

[17] a) N. Baltzer, L. Macko, S. Schaffner, M. Zehnder, *Helv. Chim. Acta* **1996**, *79*, 803–812; b) S. Schaffner, L. Macko, M. Neuburger, M. Zehnder, *Helv. Chim. Acta* **1997**, *80*, 463–471; c) S. Liu, J. F. K. Müller, M. Neuburger, S. Schaffner, M. Zehnder, *J. Organomet. Chem.* **1997**, *549*, 283–293; d) S. Schaffner, J. F. K. Müller, M. Neuburger, M. Zehnder, *Helv. Chim. Acta* **1998**, *81*, 1223–1232; e) S. Liu, J. F. K. Müller, M. Neuburger, S. Schaffner, M. Zehnder, *Helv. Chim. Acta* **2000**, *83*, 1256–1267.

[18] For recent work on the analysis of NMR spectra of [(allyl)Pd] complexes, see: a) P. S. Pregosin, R. Salzmann, *Coord. Chem. Rev.* **1996**, *155*, 35–68; b) S. Hansson, P.-O. Norrby, M. P. T. Sjögren, B. Åkermark, M. E. Cucciolito, F. Giordano, A. Vitagliano, *Organometallics* **1993**, *12*, 4940–4948; c) R. Malet, M. Moreno-Mañas, F. Pajuelo, T. Parella, R. Pleixats, *Magn. Res. Chem.* **1997**, *35*, 227–236.

[19] The *exo*:*endo* ratio is relatively insensitive to the solvent, ranging from 6:1 in $CDCl_3$ to 11:1 in [$D_6$]DMSO (T. D. Weiß, unpublished observations).

[20] Values of spin-spin coupling constants for *trans* and *cis* allylic protons are ≈12 Hz and 8 Hz, respectively. Coupling constants between $^{31}$P and $^1$H nuclei are larger in *anti* ($^3J$(H,P) ≈ 10 Hz) than in *syn* position ($^3J$(H,P) ≈ 6 Hz). See also: a) B. L. Shaw, N. Sheppard, *Chem. Ind.* **1961**, 517–518; b) J. Powell, B. L. Shaw, *J. Chem. Soc. A* **1967**, 1839–1851; c) H. C. Clark, M. J. Hampden-Smith, H. Rüegger, *Organometallics* **1988**, *7*, 2085–2093.

[21] The terms *exo* and *endo* refer to the orientation of the central allylic proton with respect to the substituent at C4 of the dihydrooxazole moiety. The descriptors *cis* and *trans* refer to the position of the higher substituted allylic terminus relative to phosphorus.

[22] a) J. Jeener, B. H. Meier, P. Bachmann, R. R. Ernst, *J. Chem. Phys.* **1979**, *71*, 4546; b) C. L. Perrin, T. J. Dwyer, *Chem. Rev.* **1990**, *90*, 935–967.

[23] a) J. Vázquez, B. Goldfuss, G. Helmchen, *J. Organomet. Chem. J. Organomet. Chem.* **2002**, *641*, 67–70; b) B. Goldfuss, U. Kazmaier, *Tetrahedron* **2000**, *56*, 6493–6496; c) M. Svensson, U. Bremberg, K. Hallman, I. Csöregh, C. Moberg, *Organometallics* **1999**, *18*, 4900–4907.

[24] a) F. Delbecq, C. Lapouge, *Organometallics* **2000**, *19*, 2716–2723; b) F. Robert, F. Delbecq, C. Nguefack, D. Sinou, *Eur. J. Inorg. Chem.* **2000**, 351–358; c) V. Branchadell, M. Moreno-Mañas, F. Pajuelo, R. Pleixats, *Organometallics* **1999**, *18*, 4934–4941; d) H. Hagelin, B. Åkermark, P.-O. Norrby, *Chem. Eur. J.* **1999**, *5*, 902–909; e) P. E. Blöchl, A. Togni, *Organometallics* **1996**, *15*, 4125–4132.

[25] a) A. Aranyos, K. J. Szabo, A. M. Castano, J.-E. Bäckvall, *Organometallics*, **1997**, *16*, 1058–1064; b) T. Suzuki, H. Fujimoto, *Inorg. Chem.* **1999**, *38*, 370–382.

[26] K. J. Szabo, *Chem. Soc. Rev.* **2001**, *30*, 136–143.

[27] Gaussian 98, Rev. A7, M. J. Frisch, G. W. Trucks, H. B. Schlegel, G. E. Scuseria, M. A. Robb, J. R. Cheeseman, V. G. Zakrzewski, J. A. Montgomery, Jr., R. E. Stratmann, J. C. Burant, S. Dapprich, J. M. Millam, A. D. Daniels, K. N. Kudin, M. C. Strain, O. Farkas, J. Tomasi, V. Barone, M. Cossi, R. Cammi, B. Mennucci, C. Pomelli, C. Adamo, S. Clifford, J. Ochterski, G. A. Petersson, P. Y. Ayala, Q. Cui, K. Morokuma, D. K. Malick, A. D. Rabuck, K. Raghavachari, J. B. Foresman, J. Cioslowski, J. V. Ortiz, B. B. Stefanov, G. Liu, A. Liashenko, P. Piskorz, I. Komaromi, R. Gomperts, R. L. Martin, D. J. Fox, T. Keith, M. A. Al-Laham, C. Y. Peng, A. Nanayakkara, C. Gonzalez, M. Challacombe, P. M. W. Gill, B. Johnson, W. Chen, M. W. Wong, J. L. Andres, C. Gonzalez, M. Head-Gordon, E. S. Replogle, J. A. Pople, Gaussian, Inc., Pittsburgh PA, **1998**.

[28] The LanL2DZ basis sets were augmented with diffuse s, p (P,Pd) and d (Pd) functions (addition of outermost function multiplied by 0.25) and polarization d function for P (exp. 0.34) and an f function for Pd (exp. 1.472): a) P. J. Hay, W. R. Wadt, *J. Chem. Phys.* **1985**, *82*, 270; b) A. W. Ehlers, M. Böhme, S. Dapprich, A. Gobbi, A. Höllwarth, V. Jonas, K. F. Köhler, R. Stegmann, A. Veldkamp, G. Frenking, *Chem. Phys. Lett.* **1993**, *208*, 111–114; c) S. Huzinaga in *Gaussian Basis Sets for Molecular Calculations*, Elsevier, Amsterdam, **1984**.

[29] a) A. D. Becke, *J. Chem. Phys.* **1993**, *98*, 5648 – 5652; b) C. Lee, W. Yang, R. G. Parr, *Phys. Rev. B* **1988**, *37*, 785 – 789.
[30] M. T. Cances, V. Mennucci, J. Tomasi, *J. Chem. Phys.* **1997**, *107*, 3032 – 3041.
[31] a) R. Prétôt, G. C. Lloyd-Jones, A. Pfaltz, *Pure Appl. Chem.* **1998**, *70*, 1035 – 1040; b) R. Prétôt, A. Pfaltz, *Angew. Chem.* **1998**, *110*, 337 – 339; *Angew. Chem. Int. Ed.* **1998**, *37*, 323 – 325.
[32] P. R. Auburn, P. B. Mackenzie, B. Bosnich, *J. Am. Chem. Soc.* **1985**, *107*, 2033 – 2046.
[33] A. Togni, *Tetrahedron Asymmetry* **1991**, *2* , 683 – 690.
[34] J. M. J. Williams, *Synlett* **1996**, 705.
[35] A. Sudo, K. Saigo, *J. Org. Chem.* **1997**, *62*, 5508.
[36] P. A. Evans, T. A. Brandt, *Org. Lett.* **1999**, 1563 – 1565.
[37] This argument only pertains to unsymmetrical ligands. It does not mean that differing bond lengths are a general cause of regioselectivity or indication of an early transition state. For *N,N* or *P,P* ligands other effects can be operative, see: P. Dierkes, S. Ramdeehul, L. Barloy, A. De Cian, J. Fischer, P. C. J. Kamer, P. W. N. M. van Leeuwen, J. A. Osborn, *Angew. Chem.* **1998**, *110*, 3299 – 3301; *Angew. Chem. Int. Ed.* **1998**, *37*, 3116 – 3118.
[38] M. Peer, J. C. de Jong, M. Kiefer, T. Langer, H. Rieck, H. Schell, P. Sennhenn, J. Sprinz, H. Steinhagen, B. Wiese, G. Helmchen, *Tetrahedron* **1996**, *52*, 7547 – 7583.
[39] G. M. Sheldrick, **1996**, unpublished work, based on a method described in R. H. Blessing, *Acta Crystallogr. Sect. A* **1995**, *51*, 33 – 38.
[40] G. M. Sheldrick, Bruker Analytical X-Ray-Division, Madison, WI, **1995**.

Received: January 7, 2002 [F3783]

  0947-6539/02/0814-3114 $ 17.50+.50/0 